Journal of Materials Processing Technology 240 (2017) 305–313

Contents lists available at ScienceDirect

Journal of Materials Processing Technology

journal homepage: www.elsevier.com/locate/jmatprotec

Methodology for predicting the angular distortion in multi-pass butt-joint welding

Paulo Cezar Adamczuk*, Ivan Guerra Machado, Jose Antonio Esmerio Mazzaferro

Federal University of Rio Grande do Sul – UFRGS, PPGE3M/LS&TC, Porto Alegre, Rio Grande do Sul, Brazil

ARTICLE INFO

Article history:
Received 19 May 2016
Received in revised form
26 September 2016
Accepted 5 October 2016
Available online 6 October 2016

Keywords:
Angular distortion prediction
Multi-pass welding
Butt-join
V- groove
Analytical-experimental model

ABSTRACT

The study was developed based on experimental evidences, by analyzing the behavior of angular distortion along the passes performed. The investigation involved ASTM A36 structural steel Plates 16 and 19 mm thick multi-pass butt-welded (V-groove) by GMAW process. The work was divided into three main groups. In each of them, experiments were performed using four different heat inputs varying between 0.6 kJ/mm and 2.5 kJ/mm. Three analytical equations were obtained for each group based on the analysis inferred about the distortion results from each experiment. The equations were used to develop a methodology for prediction of angular distortion. Three analytical models were defined and compared among themselves in order to verify the equivalence between them. One of the models obtained from one single experiment (the one that used the lowest heat input from its group) was successful on predicting angular distortion. The model allows predicting the distortion for a defined interval of heat input and number of passes within the domain in which the analytical model is valid.

1. Introduction

In V-groove butt-joint welding, the angular distortion produces geometric imprecision that difficult the structure assembling process and affects the visual and functional quality of the component. Murugan and Gunaraj (2005) stated that the restriction of the movement of the plates (in order to avoid angular distortion during welding) produces high residual stresses and, thus, may cause cracks and reduction on welded joint strength. The angular distortion consists of the rotation of the structure around the welding line and Schenk (2011) stated that it is caused by temperature gradients through the thickness of the plate. Deng et al. (2007) also reported that the temperature gradients through thickness drive the angular distortion. Zhou (1995) mentioned that angular distortion occurs in a butt joint when the transverse shrinkage is not uniform in the thickness direction. Nagy (2012) asserted that the elastic contraction on the top is larger than at the bottom and this causes the angular distortion. TWI (2016) discusses the influence of the number of passes on the angular distortion. In single V butt joint, a large single weld deposit produces less angular distortion than if the weld is made with a number of small passes. In addition, the degree of angular distortion is approximately proportional to the number of passes. Kou (2003) explains that the angular distortion increases with the thickness of the plate because of increasing amount of the weld metal, hence, increasing shrinkage forces. Moreover, for a same groove angle and a same heat input, the number of passes increases with increasing thickness, contributing to increasing the angular distortion. Pilipenko (2001) pointed out that a substantial part of the angular distortion occurs when the material is exposed to high temperatures (higher than 1000 °C for steels) and finishes well before the structure completely cools down. Therefore, if the joint is restricted to these temperatures, the weld metal undergoes plastic deformation, reducing the distortion. However, Bachorski et al. (1999) mentioned that for single V-groove butt joint, the angular distortion occurs due to linear contraction forces when the weld metal is cooled below 800 °C.

In the multi-pass butt-welding with V-groove without external restraints, the main factors contributing to the angular distortion are: the longitudinal welding cross section area that resists to the transverse shrinkage force; transient temperature field; temperature gradients through the thickness and Young's modulus. All of these factors and the angular distortion are modified as the weld beads are deposited in the joint. In bead-on-plate welding, all these factors change with the variation of the plate thickness and heat input, which in the final analysis are the main responsible for the angular distortion. Based on the work of other investigators, Wang et al. (2008) analyzed the influence of the heat input and

* Corresponding author.
E-mail addresses: paulocezar@utfpr.edu.br, pcaadamczuk@gmail.com (P.C. Adamczuk), welder@ufrgs.br (I.G. Machado), mazza@ufrgs.br (J.A.E. Mazzaferro).

http://dx.doi.org/10.1016/j.jmatprotec.2016.10.006
0924-0136/

plate thickness on the angular distortion in bead-on-plate welding. The angular distortion is significantly affected by the change in these two parameters, because they alter the transient temperature field, temperature gradient through the plate thickness and the plate stiffness (Young's modulus). Okano et al. (2011) observed that when the heat input is small, the stiffness due to thickness plate prevents the distortion in bead-on-plate welding. In contrast, when the heat input is large, the temperature gradient through the plate thickness becomes uniform and, therefore, the angular distortion is smaller. The maximum angular distortion is produced when the temperature gradients are higher and when the rigidity of the plate is low due to higher temperatures (low Young's modulus). Similar results of the angular deformation behavior with the heat input were also obtained by Tian et al. (2014) in bead-on-plate welding by the TIG process. Although there are differences between the weld beads geometry deposited in bead-on-plate and single V-groove butt joint, in both, the distortion behavior depends on the heat input and on thickness. However, in single V-groove butt joint, the distortion is related to the weld cumulative thickness, whereas in the bead-on-plate it is related to the plate thickness.

The prediction of angular distortion is crucial when the intent is to minimize its negative effects. Basically, there are three methods for predicting distortions: experimental, analytical, and numerical methods, the latter by means of the finite element method (FEM).

The use of FEM to predict distortion is used in two main approaches. The first and already consolidated, thermo-elastic-plastic is used for simple structures because of its high computational needs. The second method uses linear elastic analysis to determine the final distortion and it is used for the simulation of large welded structures, once it requires less computational time.

Recent studies have been conducted in order to predict or control welding distortion and residual stresses based in classical thermo-elastic-plastic FEM. Long et al. (2009) investigated distortions and residual stresses induced in butt joint of thin plates using GMAG welding process, modeling thermal and mechanical behavior using thermos-elastic-plastic FEM. Souto et al. (2015) proposed three transient thermal tensioning methods to minimize the out-of-plane distortion in T-fillet welded joints. These researchers used the thermo-elastic-plastic (FEM) approach for the simulation of the physical process. Manurung et al. (2013) investigated the welding sequence effect on angular distortion using FEM and experiments in butt joint and T-Fillet GMAW welding using low manganese carbon steel plates The simulation was performed using SYSWELD that allows to simulate complex welding processes. Gannon et al. (2010) investigated the influence of welding sequence on residual stress and distortion in flat-bar stiffeners in ship hull construction. The finite element method using ANSYS package was used to simulate the thermo-elastic-plastic behavior and to compare with experimental data. Tian et al. (2014) developed a neural network model for the prediction of the angular distortion and transverse shrinkage produced in GTAW bed-on-plate welding process of 304L stainless steel. The network model was compared with simulation using thermo-elastic-plastic finite element model and experiments. In this work, the researchers also investigated the effects of welding parameters including voltage, current and welding speed on the transverse and angular distortions. The results revealed that the angular distortion increases with the increasing of heat input to reach a maximum value, but decreases with further increasing of the heat input. The research revealed that the neural network can accurately predict transverse and angular distortions. Thus, the neural network model can be used to select the appropriate input welding parameters, in order to control final distortion.

Welded complex structures demand high computational time to predict distortion and residual stresses. Thus, some simplified methods using (FEM) have been developed in order to reduce the computational time required. Generally, these methods use linear elastic analysis to calculate the final distortion and the main ones are the following: (1) Inherent strains; (2) plasticity based distortion analysis; (3) Shrinkage Volume Method. Jang et al. (2007) mentioned that the inherent strains are the plastic strains arising of welding process and they are considered the source of the welding distortions and residual stresses. Luo et al. (1997) demonstrated the formation of plastic strain (inherent strains) using a model consisting of a bar and a spring at the end of the bar, which acts as an elastic constraint for deformation of the bar. In this model the magnitude of plastic strain is directly related to the maximum temperature reached at the bar and with the level of restriction imposed by the spring. Seo and Jang (1999) proposed a new method combining experimental method, analytical method and numerical method for prediction of welding deformations. In this new method, the researchers used the inherent strain theory to determine the plastic strain in the weld region using (FEM). According to these researchers, the welded joint is divided into three parts: welded region, material softening region and the base metal region. The welded region is where the plastic strains occur and plastic strains remain (inherent strain region). In the softening region around the inherent strain region the properties are changed, but plastic strains do not occur. In the base metal region, the material properties can be considered unchanged and it remains in elastic range. Barsoum et al. (2015) assessed and compared three approaches of inherent strain method for prediction of welding induced distortion on T-fillet welded structures. The results of inherent strains were compared with the elastic-plastic analysis and experiments and presented good agreement. Khurram and Shehzad (2012) applied the inherent strain theory and the equivalent load method for prediction of residual stresses and distortions in welded butt joints. An elastic FEM analysis was carried out using these equivalent loads to simulate distortions and the residual stresses. The main advantage of inherent strain method is that requires only elastic analysis (FEM) for predicting welding distortion. Jung and Tsai (2004) investigated the relationship between cumulative plastic strains and angular distortion for fillet welded thin plate T-joints. This method was solved by numerical procedure and consists of two stages. In the first stage, the cumulative plastic strain was determined using thermal-elastic-plastic analysis. While in the second stage, the angular distortion was calculated by using elastic linear analysis and using the results of plastic strain obtained in firs stage. Bachorski et al. (1999) developed the shrinkage volume method which assumes that linear thermal contraction is the main force that produces the angular distortion in the welding of single V-groove butt joints. This method was modeled using linear elastic finite-element technique and without the need to determine the transient temperatures. For these reasons, the model solution times are reduced significantly.

Although numerical methods with reduced computational requirements are available, the prediction of angular distortion through these methods presents great difficulty. According to Barroso et al. (2010) this fact is due to the high complexity of the welding phenomenon and the non-linearity involved in the thermal and structural analysis, making it difficult their practical applications. Thus experimental and analytical and statistical methods have become a viable alternative for prediction of distortion. Muragan and Gunaraj (2005) used a statistical method to develop mathematical models to correlate the angular distortion with welding process parameters. Experiments were performed to establish the relationship between process variables and the angular distortion using multi-pass GMAW process. Sudhakaran et al. (2012) proposed a method or optimization of welding process parameters using particle swarm optimization, with the aim to minimize angular distortion in stainless steel plate by GTAW Process. The experiments were conducted using design of experiments and a mathematical model was developed correlating the pro-

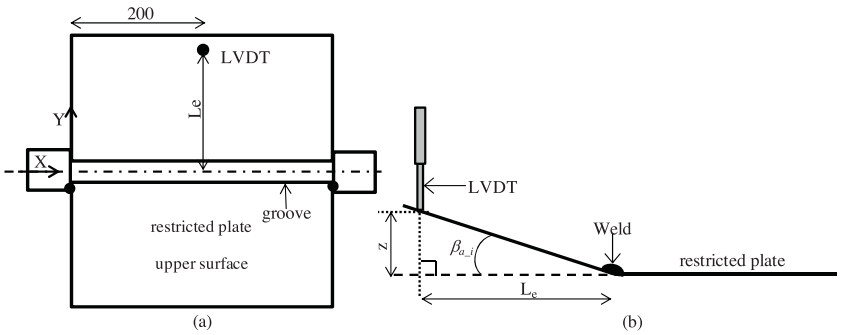

Fig. 1. (a) LVDT positioning on the specimen and (b) geometric details of the relation between linear displacement (z) and angular distortion ($\beta_{a\cdot i}$).

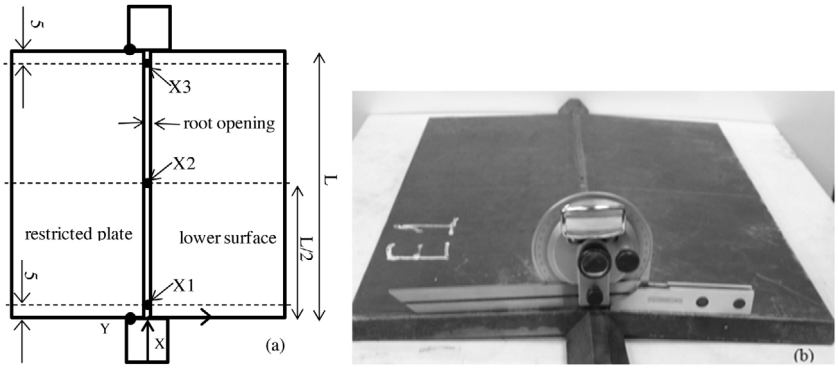

Fig. 2. (a) Dotted lines going through X1, X2 and X3 show the position of the measurements; (b) Measurement details using a goniometer.

cess parameters with the angular distortion. For the optimization procedure, the angular distortion was used as the objective function. Ramani and Velmurugan (2014) used a statistical method to develop a mathematical model to predict angular distortion in butt joint using GMAW MIG welding process parameters. Verhaeghe (1999) carried out a critical review of the main analytical models available in the literature for prediction of the weld distortion that were developed by many researchers in the last decades. The models were developed based on theoretical and empirical information and none of them are fully applicable. Therefore, they must be used under certain welding specific conditions. Based on studies conducted by another researcher, Radaj (1992) presented an analytical model to predict the angular distortion which can be used in any single pass joint or in multi-pass butt-welded joints. This model takes into account the influence of welding speed, weld pass thickness or plate thickness and heat input for determination of the angular distortion.

The main purpose of this study was to develop a methodology to predict angular distortion in multi-pass butt-joint (V-groove) welding. Such methodology was based on experimental evidences and analysis, which were focused on two main approaches. In the first approaches was analyzed the angular distortion behavior along the passes performed, for different heat inputs. In the second approaches was analyzed the direct influence of the heat input on the final distortion.

2. Experimental procedures

Specimens of ASTM A36 structural steel were welded using V-groove butt-joints with the following geometrical characteristics: 60° groove angle, 1.2 mm root opening, and 2.0 mm root face. The experiments were classified into three main groups according to their key dimensions (length × width × thickness in mm): group 1–400 × 300 × 16; group 2–400 × 300 × 19; group 3–400 × 200 × 19.

During the welding process, the angular distortion was measured using a LVDT (Linear Variable Differential Transformer) linear displacement sensor. The sensor was placed at a distance L_e from the welding line, as shown by Fig. 1(a). To allow the correct measurement, just the plate opposite to LVDT position was restricted. Considering that the distortions were measured by LVDT as linear displacement as shown in Fig. 1(b), the cumulative angular distortion up to an i-th pass ($\beta_{a\cdot i}$ in radians) was established through the relation $\beta_{a\cdot i} = \pi/180 \arctan(z/L_e)$, where L_e is the distance from the center of the weld to the LVDT position before distortion and z is the accumulated linear distance (distortion). The individual distortion of an i-th pass (β_i) may be determined by the $\beta_i = \beta_{a.i} - \beta_{a.(i-1)}$ equation, where $\beta_{a.i}$ and $\beta_{a.(i-1)}$ are angular distortions accumulated between the current and previous passes, respectively.

Aiming to verify the final angular distortion results obtained using LVDT, another measurement was made after welding. For this procedure, a goniometer with a resolution of five minutes was used (Fig. 2(b)). The measurements were made using as reference the three dotted lines at positions X1, X2 and X3 (Fig. 2(a)).

All the specimens were welded using GMAW process. The following conditions were employed for all the experiments: 20 mm contact-tube-to-work distance (CTWD) for root passes and 18 mm for filler passes; and a 75° torch longitudinal angle, backhand technique (pulling the torch). As shielding gas, a mixture of 90% Ar and 10% CO_2 using a 15 L/min flow rate was used. AWS ER70S-6 solid wire (1.2 mm gauge) was used as filler metal. The inter-pass temperature of groups 1 and 2 was kept at 50° C and, in group 3 it was kept at 100° C.

The welding conditions (current, voltage and wire feed speed) that were employed in all experiments are shown in Table 1. It can be noticed that welding conditions used in root passes are different from the ones used in filler passes.

The four nominal heat inputs employed in each group refer to filler passes. Those heat inputs were obtained by using four welding speeds, so voltage and current were kept constant in all experi-

Table 1
Welding conditions in the experiments.

	Voltage – U (V)	Current – I (A)	Wire feed speed – v_w (m/min)	contact-tube-to-work distance – CTWD (mm)
Root pass	24	265	7.7	20
Filler passes	25	275	7.7	18

Table 2
Weld speed and heat input used in the filler passes for the four groups. – Length x Width x Thickness (L x W x T).

Groups	DimensionsL × W × T(mm)	Welding travel speeds – v (mm/s)				Nominal heat inputs (Experiments) – E (kJ/mm)			
		v_1	v_2	v_3	v_4	E1	E2	E3	E4
Group 1	400 × 300 × 16	11.0	8.0	5.0	3.0	0.6	0.8	1.3	2.3
Group 2	400 × 200 × 16	11.0	8.0	5.0	3.0	0.6	0.8	1.3	2.3
Group 3	400 × 300 × 19	9.7	7.6	5.5	2.8	0.7	0.9	1.2	2.5
Group 4	400 × 200 × 19	9.7	7.6	5.5	2.8	0.7	0.9	1.2	2.5

ments, as shown previously in Table 1. Table 2 shows the welding speeds (v_1, v_2, v_3 and v_4) and the heat inputs (E1, E2, E3 and E4) in each group. As for root pass, a 0.6 kJ/mm nominal heat input was used in all experiments, as well as a welding speed (v) of 10.5 mm/s.

The equation used for the calculation of the nominal heat input (E) of the performed experiments, in J/mm, is given by Eq. (1).

$$E = \frac{U.I}{v} \quad (1)$$

3. Results and discussions

3.1. General results regarding angular distortion

This section presents the results of experiments relative to angular distortion behavior as the passes are performed. Because the angular distortion presented similar behavior for all the groups, only the results of groups 1 and 2 were presented in Figs. 3 and 4, for this purpose, two graphs were made for each group. The first graph represents the angular distortion behavior as a function of the weld passes sequence and heat inputs ($\beta_i = f(i, E)$). The second graph shows the cumulative angular distortion behavior as a function of the weld passes sequence and heat inputs ($\beta_{a\cdot i} = f(i, E)$), where β_i is the angular distortion at the i-th pass; $\beta_{a.i}$ is the cumulative distortion up to an i-th pass; and E is the nominal heat input.

Considering Figs. 3 e, 4 (groups 1 and 2), it is possible to observe that the angular distortions present similar behavior, which is also observed in group 3. This phenomenon is probably related to the gradual increase of the weld thickness as the passes are deposited, causing changes in the transient temperature field, temperature gradients and Young's modulus through the weld thickness.

In the two initial passes, the angular distortion (β_i) presented low magnitude. This phenomenon is possibly related to low temperature gradients through the thickness, which prevents a higher distortion, despite the low resistance to deformation in this situation (low weld thickness and low Young's modulus).

In the third pass, a significant increase of the distortion (βi) occurs, reaching its maximum magnitude in the fourth pass. This phenomenon is probably associated with the: increase of the temperature gradients through the thickness and low Young's modulus due to high temperatures at the weld root lower surface.

From the fifth pass onwards, the angular distortion (β_i) gradually decreases, tending to drop to an insignificant value in the experiments involving large numbers of passes (lower heat inputs). This phenomenon is probably associated with the gradual increase of the weld thickness, which reduces the temperature at the lower surface of the plate, weld root and, consequently, increases the Young's modulus through the thickness. The combined effects of the increased thickness and Young's modulus progressively increase the resistance to deformation as the passes are made (gradual increase in stiffness).

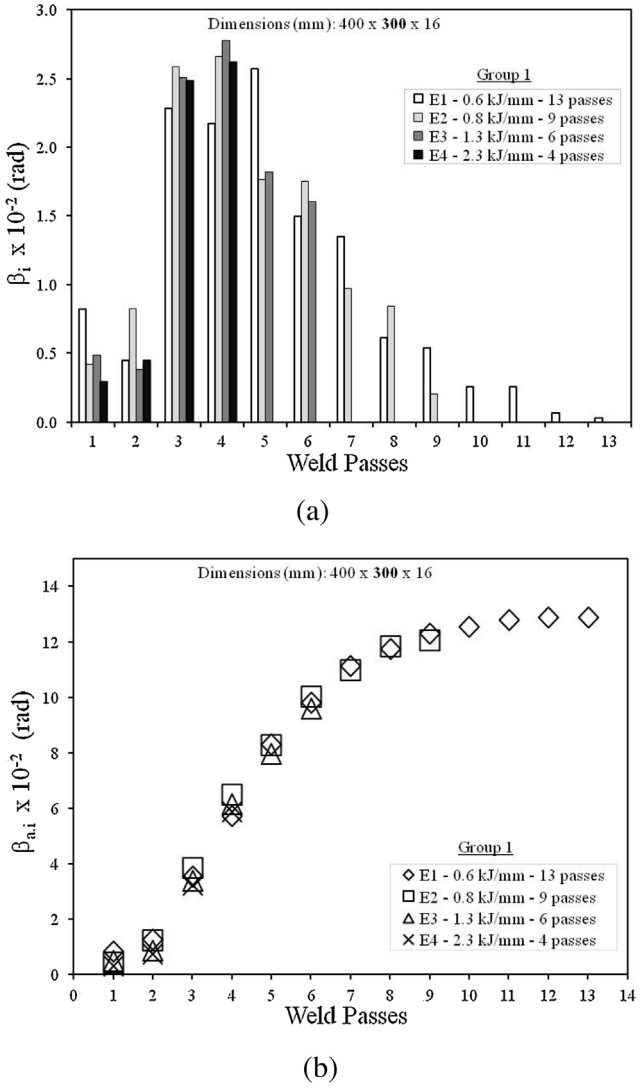

Fig. 3. Relation between the angular distortion and the weld passes sequence for all heat inputs of group 1. (a) β_i (individually at the i-th pass) and (b) $\beta_{a\cdot i}$ (accumulated until an i-th pass).

3.1.1. Analysis of the average angular distortions

Because the angular distortions (β_i and $\beta_{a\cdot i}$) present approximately constant values at a specific pass, regardless the heat input

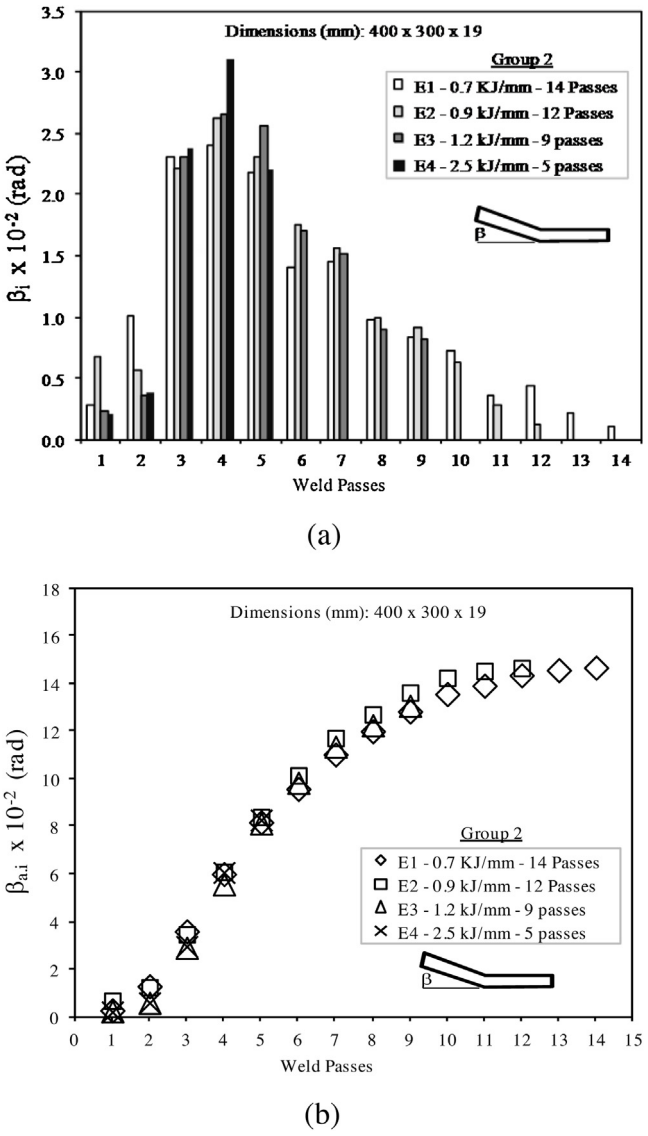

Fig. 4. Relation between the angular distortion and the weld passes sequence for all heat inputs of group 2. (a) βi (individually at the i-th pass) and (b) βa.i (cumulated until an i-th pass).

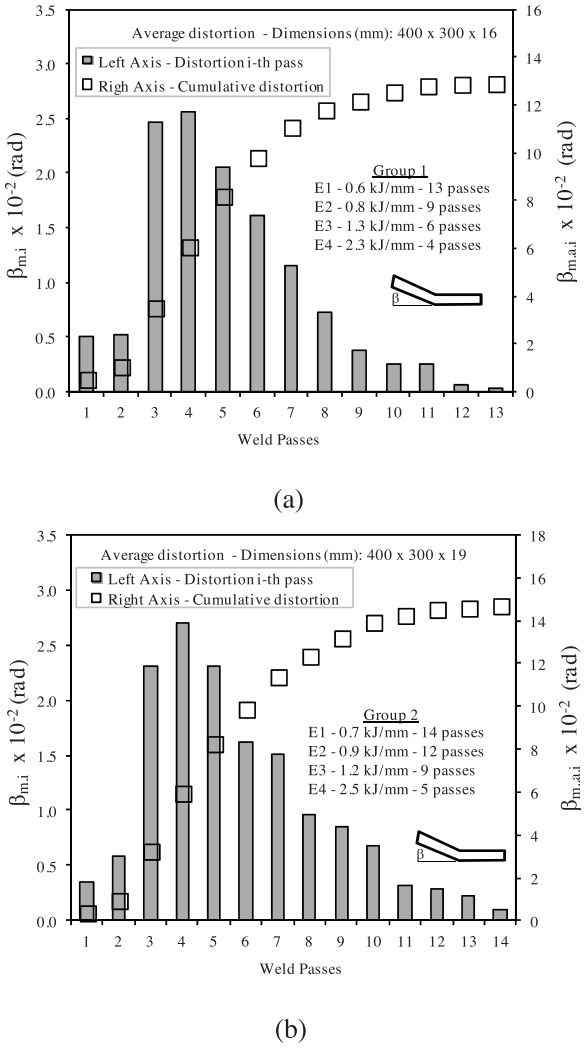

Fig. 5. Average angular distortion as a function of the weld passes sequence, in (a) group 1 and (b) group 2.

involved, the angular distortion behavior can be evaluated by using only their average values. Therefore, the average angular distortion for the i-th pass ($\beta_{m\cdot i}$) and the cumulative distortion up to an *i*-th pass ($\beta_{m\cdot a\cdot i}$) can be determined by Eqs. (2) and (3), respectively:

$$\beta_{m.i} = \frac{1}{n}\sum_{j=1}^{n}\beta_{i,j} \tag{2}$$

$$\beta_{m.a.i} = \frac{1}{n}\sum_{j=1}^{n}\beta_{a.i} \tag{3}$$

where i = [1,2,. . ., N_p] and N_p is the total number of passes for the experiment with the lowest heat input of the analyzed group; j = [1,2,.., n] and *n* is the number of heat inputs of the *i*-th pass analyzed. Therefore, the graphs of Fig. 5 represent the average angular distortion behavior as a function of the weld passes sequence for groups 1 and 2.

Despite the fact that the results for group 3 were omitted, their behavior is similar to those of groups 1 and 2. Through bars, the left axis of these graphs represents the average angular distortion taking place at each pass ($\beta_{m.i}$). On the other hand, through markers, the right axis shows the average cumulative angular distortion ($\beta_{m\cdot a\cdot i}$), where the indexes *m* and *a* represent the average and cumulative values, respectively.

In order to make practical use of the results from the graphs in Fig. 5 for the development of a new methodology to predict angular distortion, a curve that best represents the behavior of the average cumulative angular distortion as a function of the number of weld passes performed was fitted. For convenience, it was established that i = N and $\beta_{m\cdot a\cdot i} = \beta_{m.g}$, $\beta_{m\cdot g}$, therefore assuming $\beta_{m\cdot g} = f(N)$ as the functional relationships, where *N* denotes the number of passes made in each group of experiment, and *g* indicates the group. The curve fitting was made excluding the root pass because its heat input differs from the filler passes, obtaining, as a result of that, a better correlation.

Moreover, as seen in Figs. Fig. 33(b) and Fig. 44(b), in the experiments involving low heat inputs (0.6 kJ/mm and 0.7 kJ/mm), the cumulative distortion has an insignificant variation in the last passes. Therefore, to improve the fitting quality, three more passes were added at the end, keeping in them the last pass distortion. The curves were adjusted by using the least square method. The analytical equations that better represent the relation between the angular distortion and the numbers of deposited passes are third-order polynomial functions, as shown in Eqs. (4)–(6).

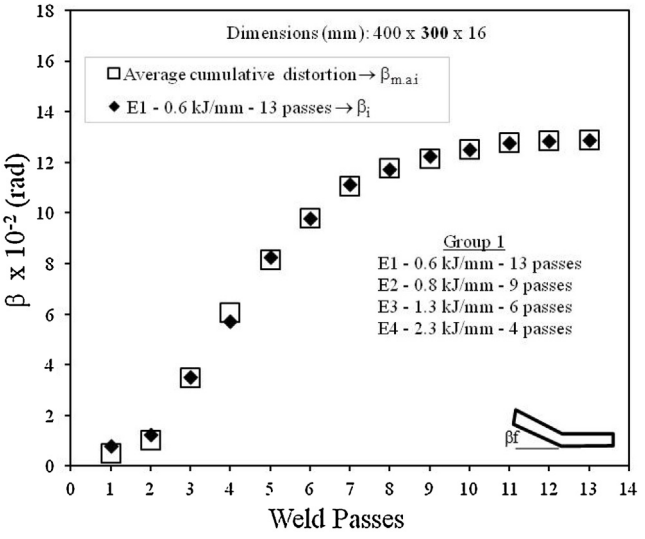

Fig. 6. Comparison between average cumulative angular distortion ($\beta_{m\cdot a\cdot i}$) and the cumulative angular distortion ($\beta_{a\cdot i}$) of the experiment with the greatest number of passes (group 1).

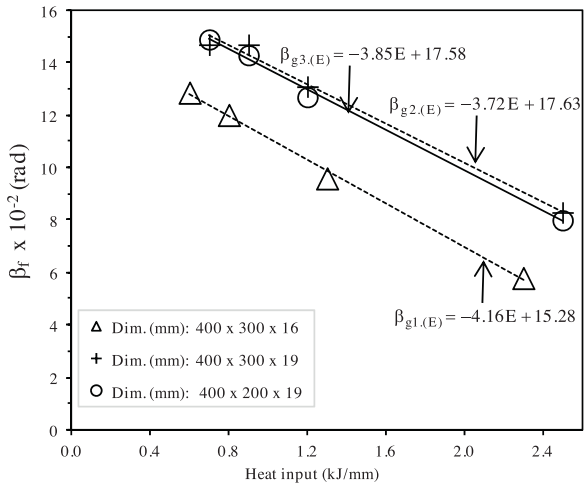

Fig. 7. Final angular distortion (β_f) as a function of the heat input (E) for two plate thicknesses (16 mm for groups 1; and 19 mm for groups 2 and 3).

The Person correlation coefficients (r) obtained for the three groups was 0.999, indicating that the third-order polynomial equations represent an excellent fitting. The *g1*, *g2* and *g3* indexes presented in the equations refer to the experimental groups 1, 2 and 3, respectively. For group 1, the equations are valid for the N = [2,3,. . .,14] pass interval, whilst for groups 2 and 3, for the N = [2,3,. . ., 15] pass interval.

$$\beta_{m.g1} = 0.0083N^3 - 0.33N^2 + 4.46N - 6.8 \quad (4)$$

$$\beta_{m.g2} = 0.0056N^3 - 0.264N^2 + 4.11N - 6.55 \quad (5)$$

$$\beta_{m.g3} = 0.0047N^3 - 0.23N^2 + 3.673N - 4.962 \quad (6)$$

3.1.2. Distortion analysis at lower heat input

For the different groups of experiments studied, the average cumulative distortion ($\beta_{m\cdot a\cdot i}$) presented behavior similar to the cumulative distortion of the experiment at lowest heat input (higher number of passes). This fact can be checked by analyzing group 1 experiments, Fig. 6.

Therefore, as in Section 3.1.1, the analytical expression was once again fitted to better represent the behavior of the cumulative angular distortion as a function of the number of passes in the experiment with the lowest heat input. Again, to improve the curve fitting quality, the analysis excluded the root pass and three passes with the same accumulated distortion of the last pass were added at the end. Therefore, the obtained expressions, which better represent the angular distortion behavior, are third-order polynomial functions, as defined by Eqs. (7)–(9). The correlation coefficients, r, obtained were, respectively: $r_1 = 0.998$, $r_2 = 0.999$ and $r_3 = 0.999$; showing that the obtained equations represent an excellent fitting. The *g1*, *g2* and *g3* refer to groups (1), (2) and (3), respectively; and the e_1 index refers to the experiment with the lowest heat input and the highest number of passes for each group. For group (1), the equations are valid for the N = [2; 14] pass interval, whilst for groups (2) and (3), for the N = [2; 15] pass interval.

$$\beta_{g1.e1} = 0.0078N^3 - 0.32N^2 + 4.336N - 6.52 \quad (7)$$

$$\beta_{g2.e1} = 0.0045N^3 - 0.222N^2 + 3.654N - 5.29 \quad (8)$$

$$\beta_{g3.e1} = 0.004N^3 - 0.204N^2 + 3.442N - 4.314 \quad (9)$$

The third-order polynomial is more adequate when there is low heat input (heat input ≤0.7 kJ/mm) and high number of passes. In those cases, the variation of the cumulative angular distortion in the last passes becomes insignificant.

3.2. Final angular distortion (β_f)

Fig. 7 exhibits the final angular distortion behavior (β_f) as a function of the heat input for 16 mm and 19 mm plate thicknesses.

Based on the analysis of Fig. 7, it becomes evident that, for both thicknesses, the angular distortion presents a tendency of linear decrease as the heat input increases. Therefore, a linear equation was fitted ($\beta = aE + b$) using simple linear regression for each group of experiments, as presented by Eqs. (10)–(12). In the equations previously shown, $a = \Delta\beta/\Delta E$ is the slope coefficient, and b is where the straight-line intercepts the vertical β_f axis. The obtained correlation coefficients (r) were $r_1 = 0.998$, $r_2 = 0.995$, and $r_3 = 0.998$, showing an excellent fitting. It can be noticed that the slope coefficients ($\Delta\beta/\Delta E$) present similar behavior.

$$\beta_{g1.(E)} = -4.16E + 15.28 \quad (10)$$

$$\beta_{g2.(E)} = -3.72E + 17.63 \quad (11)$$

$$\beta_{g3.(E)} = -3.85E + 17.58 \quad (12)$$

3.3. Distortion prediction

Based on the results obtained from the experiments and the analyses from Sections 3.1 and 3.2, a methodology to predict angular distortion was developed considering the three groups of analytical equations, from now being referred as models A, B and C. Model A employs the group of equations from Section 3.1.1 (Eqs. (4)–(6)); model B applies Eqs. (7)–(9), from Section 3.1.2; whilst model C uses Eqs. (10)–(12), from Section 3.2. The main objective of the proposed methodology is to verify if the three models present similar results between themselves and, also, to suggest the most adequate for the prediction of angular distortion.

To implement the proposed methodology, it is necessary to establish the existing relation between the number of passes (N), welding parameters and geometrical data from the grooves. Initially, the cross-sectional area of the filler metal deposited in each pass (A_p) must be determined, which is done by Eq. (13), where d is the diameter of the wire filler metal in mm; v_w is the wire feed speed in m/min; v is the welding speed in mm/s; The constant C = 13.09 resulted from the C = 16.67(pi/4), where 16.67 is the con-

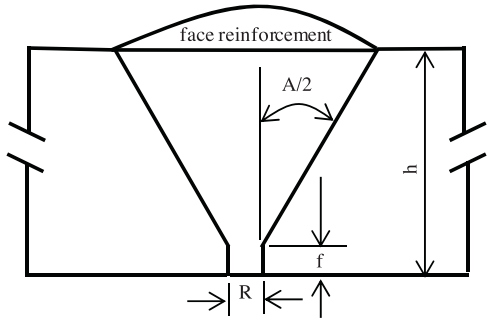

Fig. 8. V-groove butt-joint geometry used in Eq. (14).

stant used to convert the units of wire feed speed (v_w) of m/min for mm/s. The losses of metal as spatter were not considered.

$$A_p = Cd^2 \frac{v_w}{v} \tag{13}$$

In Eq. (13), the wire feed speed (v_w) is a function of the welding current (I) and of the welding wire diameter (d) that is, $v_w = f(I,d)$. Moreover, in the specific case of the performed experiments, the power source parameters (I, U, v_w) were kept constant, and the heat input changes were due the welding speed variation.

The total cross-sectional area (A_{total}) is composed by the groove and reinforcement areas and it can be calculated using Eq. (14), as shown in Fig. 8. The factor 1.2 that multiplies the whole term in brackets represents the cross-sectional reinforcement area (face reinforcement), where R is the root opening, h is the plate thickness, f is the height of the root face, and A is the groove angle in degrees (Fig. 8).

$$A_{total} = 1.2\left(Rh + \tan\left(\frac{A}{2}\right)(h-f)^2\right) \tag{14}$$

When the heat input of the root pass differs from that of the filler passes, the number of filler passes can be determined by Eq. (15), and added to the root pass to obtain the total number of passes (N) Eq. (16). The cross-sectional area of the root pass (A_{rp}) and the area of the each filler pass (A_{fp}) are determined by Eq. (13), whilst the total area, by Eq. (14).

$$N_f = \frac{(A_{total} - A_{rp})}{A_{fp}} \tag{15}$$

$$N = N_f + 1 \tag{16}$$

For the case in which the welding parameters of the root and the filler passes are the same, the total number of passes is given by Eq. (17).

$$N = \frac{A_{total}}{A_p} \tag{17}$$

Eq. (18) was obtained by combining Eqs. (13) and (15); On the other hand, Eq. (19) was obtained by combining Eqs. (13) and (17). These two equations associate the welding speed of the filler passes with the number of passes needed to completely fill the groove. Eq. (18) is used when the welding parameters of the root pass differ of the filler passes, whilst Eq. (19) is used when the welding parameters of the root and filler passes are the same.

$$v = N_f \frac{Cd^2 v_w}{(A_{total} - A_{rp})} \tag{18}$$

$$v = N \frac{Cd^2 v_w}{A_{total}} \tag{19}$$

With the aim of demonstrating the proposed methodology, Table 3 was created using the welding parameters of the group 1 as the reference. The weld passes (N) varied from 4 to 13 and, the filler passes (N_f), the from 3 to 12. Initially, it was determined the welding speeds (v) for the filler passes, using Eq. (18). After that, the respective heat inputs were calculated using Eq. (1). Finally, the angular distortions were determined by using the equations of the three proposed models, that is, Eqs. (4), (7) and (10) (group 1). Areas A_{rp}, A_{fp} and A_{total} were determined by Eqs. (13) and (14). The parameters used in these equations were the same used in the group 1 experiments, which were: $d = 1.2$ mm; $v_w = 7.7$ m/min; $R = 1.2$ mm; $f = 2.0$ mm; $A = 60°$; and $h = 16$ mm. It must be observed that the welding speed and heat input shown in Table 3, refer to the filler passes. For calculating the root pass area (A_{rp}), the welding speed of 10.5 mm/s was used.

By applying the same methodology used in Table 3, the angular distortion for groups 2 and 3 was determined. Therefore, to compare the results between the three proposed models, the angular distortion as a function of the number of passes for groups 1, 2 and 3 is graphically represented in Fig. 9. In these graphs, it is also possible to identify the welding speed and heat input. Thus, for a number of passes (N) needed to completely fill the welded joint (root pass, filler passes and reinforcement passes), it is possible to identify the respective welding speed, heat input and produced angular distortion.

As observed in Fig. 9, the three models show similar results, thus, any of them could be used to predict angular distortion. However, whilst models A and C were obtained performing four experiments, model B needed only one, being considered the most adequate model because it requires fewer tests, thereby reducing the costs involved. Nevertheless, the conclusion that model B is the most suitable for predicting the angular distortion was based on analysis of the results of the four experiments performed for each group. In these experiments, it was clear that, regardless of the heat input used, the angular distortion presented similar values for a specific weld pass, as discussed on Section 3.1. Thus, according to the analysis described in Section 3.1.2, it is possible to represent the angular distortion behavior for a group of experiments with different heat inputs, using just the experiment with the lowest heat input. For that, the heat input involved must be low enough so that, in the last two passes, the angular distortion is negligible. This heat input depends on the plate thickness, considering that in the performed experiment it ranged from 0.6 to 0.7 kJ/mm. Based on these experiments, it is advisable that the lower limit of the heat input should be determined by the relation $E = 0.036\,h$, where E is the nominal heat input in kJ/mm, and h is the plate thickness in mm. Thus, based on the lower limit of the heat input, it is also defined the upper limit of the number of passes. For the less thick plates, the heat input value in the experiment may assume reduced values, therefore, to avoid high welding speeds, it is advisable to use low welding currents.

Even if, by means of model B, the equations are valid for the pass intervals [2;14] and [2;15], as shown in Sections 3.1.1 and 3.1.2, for the prediction of angular distortion using a reduced number of passes, it would be necessary to use high heat input as upper limit. For example, using two passes performed in group 1, the heat input will reach a value of 6.9 kJ/mm. Therefore, as observed in Fig. 9, for the specific case of the performed experiments, it is recommended that the number of passes and heat input should be in the following intervals, respectively: group 1–[4; 13] and [2.3; 0.6] kJ/mm; groups 2 and 3–[5; 15] and [2.5; 0.7] kJ/mm. Thus, the lower limit of number of passes to be used in model B must be associated with technical limitations of the welding equipment.

3.1.1. Steps to implement the proposed methodology

The necessary procedures to employ model B for predicting the angular distortion are summarized by the following steps:

Table 3
Relation between the number of passes (N), welding speed (v), heat input (E) and angular distortion ($\beta_{m\cdot g1}$, $\beta_{g1\cdot e1}$ and $\beta_{g1.(E)}$) for the experiments of group 1.

N	N_f	vmm/sEq. (19)	EkJ/mmEq. (1)	$\beta_{m\cdot g1}$(rad)Eq. (4)	$\beta_{g1\cdot e1}$(rad)Eq. (7)	$\beta_{g1.(E)}$(rad)Eq. (10)
4	3	3.0	2.29	6.1	6.2	5.8
5	4	4.0	1.72	8.1	8.1	8.1
6	5	5.0	1.37	9.6	9.7	9.6
7	6	6.0	1.14	10.8	10.8	10.5
8	7	7.0	0.98	11.6	11.7	11.2
9	8	8.0	0.86	12.2	12.3	11.7
10	9	9.0	0.76	12.5	12.6	12.1
11	10	10.0	0.69	12.7	12.8	12.4
12	11	11.0	0.62	12.8	12.9	12.7
13	12	12.0	0.57	12.7	12.9	12.9

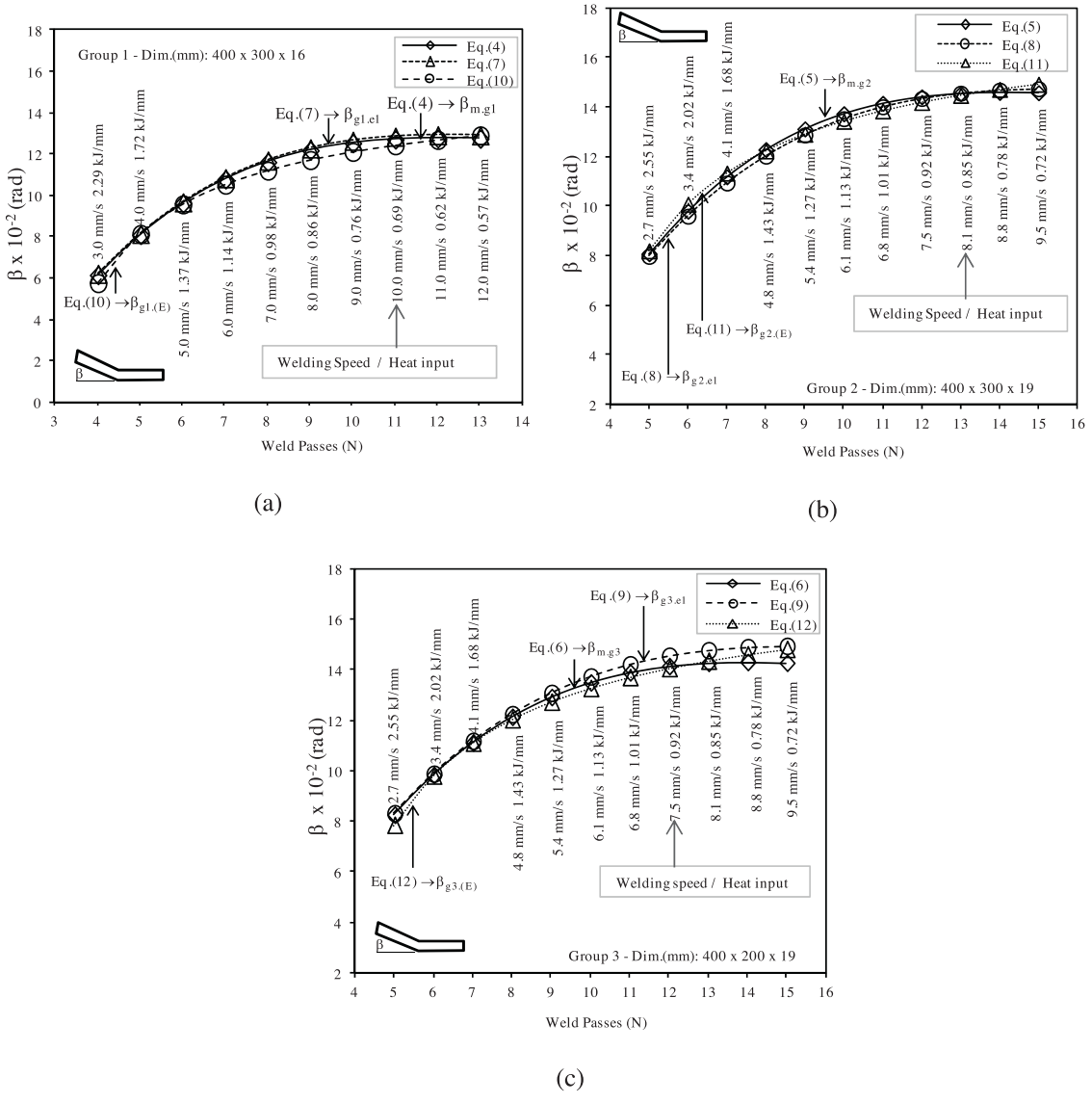

Fig. 9. Angular distortion (β) as a function of the number of passes (*N*) for the three proposed models, obtained from (a) Group 1, (b) Group 2 and (c) Group 3 experiments.

1) Define welding parameters for the power source: current (wire feed speed) and voltage;
2) Determine the heat input based on the following criteria, E = 0.036 h, and also the respective welding speed using Eq. (1);
3) Determine the number of passes using Eqs. (15) and (16) or (17);
4) Perform the experiment, measuring the cumulative angular distortion produced in each pass, and represent these distortions as a function weld passes sequence;
5) Determine the analytical equation (curve fitting) that best represents the cumulative angular distortion behavior as a function of the weld passes sequence, as previously defined in Section 3.1.2;
6) By using the same methodology employed to calculate the data in Table 3, determine for model B the existing relation between the angular distortion, number of passes, welding speed and heat input. Also, define the interval of passes and heat inputs

for which the fitted analytical equation is valid to predict the angular distortion.

4. Conclusions

The main goal of the current study was to develop a methodology to predict the angular distortion in multi-pass V-butt joint welding based on experimental evidences and analysis performed. The work was divided into three groups and experiments were performed using four heat inputs in each group. The main conclusions are summarized below:

- The angular distortion presented similar behavior for all experiments. It was found that the angular distortion along the passes, first increases to its maximum value at the fourth pass, and then decreases with the further increasing of passes. These findings have significant importance for the understanding of how the angular distortion along the passes is influenced by heat input and by stiffness produced by the previously beads deposited in the joint.
- The angular distortion produced in a given weld pass was the same for all experiments of group, regardless of heat input used in each group. This finding allowed the development of an experimental method to predict the final angular distortion.
- The prediction of the angular distortion can be made through an experimental method, using the results obtained of the accumulated angular distortion along the passes performed. These results can be used to expand the prediction of the angular distortion for an interval of heat inputs corresponding to an interval of passes, where the curve fitted of the experiment is valid (model B).
- The evidence suggests that the proposed method can also be applied in many other situations, such as welding processes, thicknesses, groove types and angles, and in situations where heat input varies with current, voltage and welding speed.

Acknowledgments

The authors would like to thank to Federal University of Technology of Paraná (UTFPR) for granting the paid educational leave to one of the authors (PCA) during the development of this research.

References

Bachorski, A., Painter, M.J., Smailes, A.J., Wahab, M.A., 1999. Finite-element prediction of distortion during gas metal arc welding using the shrinkage volume approach. J. Mater. Process. Technol. 92–93, 405–409.
Barroso, A., Cañas, J., Picón, R., París, F., Méndez, C., Unanue, I., 2010. Prediction of welding residual stresses and displacements by simplified models. Experimental validation. Mater. Des. 31, 1338–1349.
Barsoum, Z., Ghanadi, M., Balawi, S., 2015. Managing welding induced distortion – comparison of different computational approaches. Proceedings of the 1 St International Conference on Structural Integrity, 70–77.
Deng, D., Liang, W., Murakawa, W., 2007. Determination of welding deformation in fillet-welded joint by means of numerical simulation and comparison with experimental measurements. J. Mater. Process. Technol. 183, 219–225.
Gannon, L., Liu, Y., Pegg, N., Smith, M., 2010. Effect of welding sequence on residual stress and distortion in flat-bar stiffened plates. Mar. Struct. 23, 385–404.
Jang, C., Kim, D., Jo, Y.T., Ryu, Y.C., 2007. Welding distortion analysis of hull blocks using equivalent load method based on inherent strain. In: Proceedings 10 Th International Symposium on Practical Design of Ships and Other Floating Structures, Houston, Texas, USA.
Jung, G.H., Tsai, C.L., 2004. Plasticity-based distortion analysis for fillet welded thin-plate T-joints – a new relationship between cumulative plastic strains and angular distortion was found. Weld. J. 83 (6), 177–187.
Khurram, A., Shehzad, K., 2012. FE simulation of welding distortion and residual stresses in butt joint using inherent strain. Int. J. Appl. Phys. Math. 2 (6), 405–408.
Kou, S., 2003. Welding Metallurgy, second ed. Wiley Interscience, Hoboken, pp. 126–130.
Long, H., Gery, D., Carlier, A., Maropoulos, P.G., 2009. Prediction of welding distortion in butt joint of thin plates. Mater. Des. 30, 4126–4135.
Luo, Y., Murakawa, H., Ueda, Y., 1997. Prediction of welding deformation and residual stress by elastic FEM based on inherent strain. JWRI 26, 49–57.
Manurung, Y.H.P., Lidam, R.N., Rahim, M.R., Zakaria, M.Y., Redza, M.R., Sulaiman, M.S., Tham, G., Abas, S.K., 2013. Welding distortion analysis of multi-pass joint combination with different sequences using 3D FEM and experiment. Int. J. Press. Vessels Pip. 111–112, 89–98.
Murugan, V., Gunaraj, V., 2005. Effects of process parameters on angular distortion of gas metal arc welded structural steel plates. Weld. J. 84 (11), 165–171.
Nagy, T., 2012. Investigation of Thermal Techniques to Mitigate Buckling Distortion in Welded Panels PhD Thesis. Cranfield University.
Okano, S., Mochizuki, M., Yamamoto, K., Tanaka, M., 2011. An attempt to enhance numerical models of angular distortion by considering the physics of the welding arc. Weld. World 55, 93–100.
Pilipenko, A., 2001. Computer Simulation of Residual Stress and Distortion of Thick Plates in Multi-electrode Submerged Arc Welding. Their Mitigation Techniques. Doctoral Thesis. Norwegian University of Science and Technology.
Radaj, D., 1992. Heat Effects of Welding – Temperature Field, Residual Stress, Distortion. Springer, Berlin, pp. 219–222.
Ramani, S., Velmurugan, V., 2014. Effect of process parameters on angular distortion of MIG welded AI6061 plates. In: Proceedings of the 5th International and 26th All India Manufacturing Technology, Design and Research Conference, Guwahati, India, 401 (1) 401 (6).
Schenk, T., 2011. Modelling of Welding Distortion the Influence of Clamping and Sequencing Doctor Thesis. Technische Universiteit Delft.
Seo, S., Jang, C.D., 1999. A study on the prediction of deformations of welded ship structures. J. Ship Prod. 15 (2), 73–81.
Souto, J., Ares, E., Alegre, P., 2015. Procedure in reduction of distortion in welding process by high temperature thermal transient tensioning. Procedia Eng. 132, 732–739.
Sudhakaran, R., Murugan, V.V., Sakthivel, P.S., 2012. Optimization of process parameters to minimize angular distortion in gas tungsten arc welded stainless steel 202 grade plates using particle swarm optimization. J. Eng. Sci. Technol. 7 (2), 195–208.
TWI, 2016. http://www.twi-global.com/technical-knowledge/job-knowledge/distortion-prevention-by-design-034/.
Tian, L., Luo, Y., Wang, Y., Wu, X., 2014. Prediction of transverse and angular distortions of gas tungsten arc bead-on-plate welding using artificial neural network. Mater. Des. 54, 458–472.
Verhaeghe, G., 1999. Predictive Formulae for Weld Distortion – A Critical Review, first ed. Abington Publishing, Cambridge, pp. 1–90.
Wang, R., Rashed, S., Serizawa, H., Murakawa, H., Zhang, J., 2008. Study on welding inherent deformations in welded structural materials. JWRI 37, 91–100.
Zhou, Y., 1995. Analysis of Welding Distortion Using Qualitative and Semi-Quantitative Techniques: Master of Applied Science. University of British Columbia.